European Journal of Neuroscience, Vol. 17, pp. 1768–1776, 2003

γ-Frequency fluctuations of the membrane potential and response selectivity in visual cortical neurons

Maxim Volgushev,[1,2] Joachim Pernberg[1] and Ulf T. Eysel[1]
[1]Department of Neurophysiology, Ruhr-University Bochum, MA 4/149, D-44780 Bochum, Germany
[2]Institute of Higher Nervous Activity and Neurophysiology RAS, 117865 Moscow, Russia

Keywords: cat, gamma oscillations, intracellular recording, response selectivity, V1, visual cortex

Abstract

Fluctuations at frequencies of 25–70 Hz is an inherent property of cortical activity. These rapid, γ-range fluctuations are apparent in the local field potentials, in spiking of cells and cell groups, and in the membrane potential of neurons. To investigate stimulus dependence of the γ-frequency fluctuations of the membrane potential, we have recorded intracellularly responses of cells in cat visual cortex to presentation of moving gratings. We found γ-range fluctuations of the membrane potential in both simple and complex cells. The strength of the γ-frequency fluctuations correlated with the stimulus optimality. Furthermore, the amplitude of the γ-frequency fluctuations correlated with the phase of stimulus-imposed slow changes of the membrane potential. The combination of these features makes cortical neurons capable of encoding the slow changes in the visual world in a kind of amplitude modulation of the high frequency fluctuations. This assures reliable transformation of the membrane potential changes into spike responses without compromising the temporal resolution of visual information encoding in the low frequency range.

Introduction

Changes in the visual environment are encoded by visual neurons in modifications of the pattern and frequency of the action potentials. Although vigorous firing in a visual cortex cell may be evoked by slow but strong depolarization, addition of rapid fluctuations in the γ-frequency range (>25 Hz) makes translation of the membrane potential changes into spike trains a lot more precise and reliable (Mainen & Sejnowski, 1995; Nowak *et al*., 1997; Volgushev *et al*., 1998; Salinas & Sejnowski, 2000). Because of their capability to impose a narrow temporal window for the integration of synaptic inputs and to produce precisely timed sequences of action potentials in a nerve cell (Mainen & Sejnowski, 1995; Nowak *et al*., 1997; Volgushev *et al*., 1998), the γ-frequency oscillations of the membrane potential may be instrumental in synchronization of neuronal activity (Lampl & Yarom, 1993; König *et al*., 1996; Volgushev *et al*., 1998). The relationship between the γ-frequency oscillations and synchronization of activity across cells and cell populations has been investigated so far with the use of extracellular recordings of local field potentials, multiunit activity and single-cell firing (Eckhorn *et al*., 1988; Gray & Singer, 1989; Gray *et al*., 1990; Engel *et al*., 1991; Livingstone, 1996; Frien & Eckhorn, 2000). These studies have revealed that oscillations and synchronization depend on the properties of the stimulus, including its global arrangement and behavioural relevance (Engel *et al*., 1991; Vaadia *et al*., 1995; Riehle *et al*., 1997). The extracellularly recorded oscillations reflect changes in the membrane potential in individual cells and cell populations and, indeed, oscillations of the membrane potential at frequencies >20 Hz were observed during the responses to moving stimuli in neurons with complex receptive fields (Jagadeesh *et al*., 1992; Anderson *et al*., 2000b) and in a subpopulation of simple cells (Gray & McCormick, 1996). These oscillations in the visual cortical neurons are most probably of synaptic origin (Bringuier *et al*., 1997; Lampl *et al*., 1999). If γ-frequency fluctuations of the membrane potential were stimulus-dependent, this effective tool of reliable production of precise firing patterns could contribute to the response selectivity and stimulus encoding in cortical cells. The dependence of the oscillations of extracellular signals on stimulus properties (Gray *et al*., 1990; Engel *et al*., 1991; Livingstone, 1996; Frien & Eckhorn, 2000) provides an indirect support for this idea. To test this conjecture directly we made intracellular recordings from cat visual cortex and analysed the relationship between spike response selectivity and γ-frequency fluctuations of the membrane potential.

Materials and methods

Experiments were performed on nine adult cats (3.0–4.5 kg). The procedures were approved by a local animal welfare committee (Bezirksregierung Arnsberg, Germany). The details of surgery and maintenance of animals are described elsewhere (Volgushev *et al*., 2000; Volgushev *et al*., 2002). Anaesthesia was induced with a mixture of ketamine hydrochloride (Ketanest, Park-Davis GmbH, Germany; 0.3 mL/kg, i.m.) and Rompun (Bayer, Germany; 0.08 mL/kg, i.m.), and maintained during the experiment with a gas mixture of $N_2O : O_2$ (70 : 30) and 0.2–0.4% halothane (Eurim-Pharm, Germany). Surgery was started after stable anaesthesia with complete analgesia was achieved. Fluid replacement was achieved by the intra-arterial administration of 6 mL/h of Ringer solution containing 1.25% glucose. Intracellular recordings were made with sharp electrodes, filled with 2.5 M potassium acetate, resistance 70–120 MΩ. Moving gratings for visual stimulation were generated using subroutines of the Vision Works stimulation system (Cambridge Research Systems, New Hampshire, USA) and our own programs. Response selectivity was tested by presenting stimuli of different orientations (8–16) for 4–6 s in a

Correspondence: Dr M. Volgushev, [1]Department of Neurophysiology, as above.
E-mail: maxim@neurop.ruhr-uni-bochum.de

Received 16 December 2002, revised 25 February 2003, accepted 26 February 2003

doi:10.1046/j.1460-9568.2003.02609.x

pseudorandom sequence. Cells were classified as simple or complex according to standard criteria (Orban, 1984) and using the spike response modulation index, defined as a half of the peak-to-peak modulation divided by the mean increase in the spiking frequency during presentation of an optimal moving grating (Dean & Tolhurst, 1983; Skottun *et al*., 1991). This allowed correlation of the properties we have studied to the simple–complex classification.

To study the spectral composition of membrane potential responses we performed fast Fourier transformation (FFT) of 4096-ms epochs of the membrane potential traces, starting with the beginning of grating movement. Before FFT, action potentials were detected at their threshold as described in detail elsewhere (Volgushev *et al*., 2002) and removed from the membrane potential traces. The membrane potential was linearly interpolated between two points, the first one set at 0.7 ms before the detected spike threshold was reached and the second one 4.3 ms after the detected spike threshold was reached. This window of 5 ms duration safely covered the complete waveform of action potentials in our recordings (see Fig. 1). This conservative removal of the action potentials allowed us to avoid any possible contribution of action potential afterhyperpolarization and/or depolarizing afterpotentials to the power spectra of the membrane potential traces. Response components of a certain frequency band were extracted as follows. We performed an FFT of the membrane potential trace, then zeroed in the results all coefficients corresponding to the frequencies outside that given band, and then performed an inverse FFT. The low frequency range was set to cover the temporal frequency of the visual stimulation, which was 0.3–3 Hz in different cells. The high frequency component was always set to the γ-range (25–70 Hz). For quantification of the relationship between the phase of the low frequency response component and the amplitude of the γ-frequency fluctuations, we calculated a 'phase-lock coefficient'. For each data point, the value of the normalized envelope of the high frequency component was multiplied by the amplitude value of the normalized low frequency response at that point. The phase-lock coefficient was the sum of all these products. Because the low frequency component does not contain a DC shift and its mean is 0, the sign of this coefficient shows association of higher amplitudes of the high frequency envelope with the positive or negative phase of the low frequency fluctuation, and its absolute value is a measure of the strength of the phase-locking. For example, if the amplitude of the high frequency oscillation remains

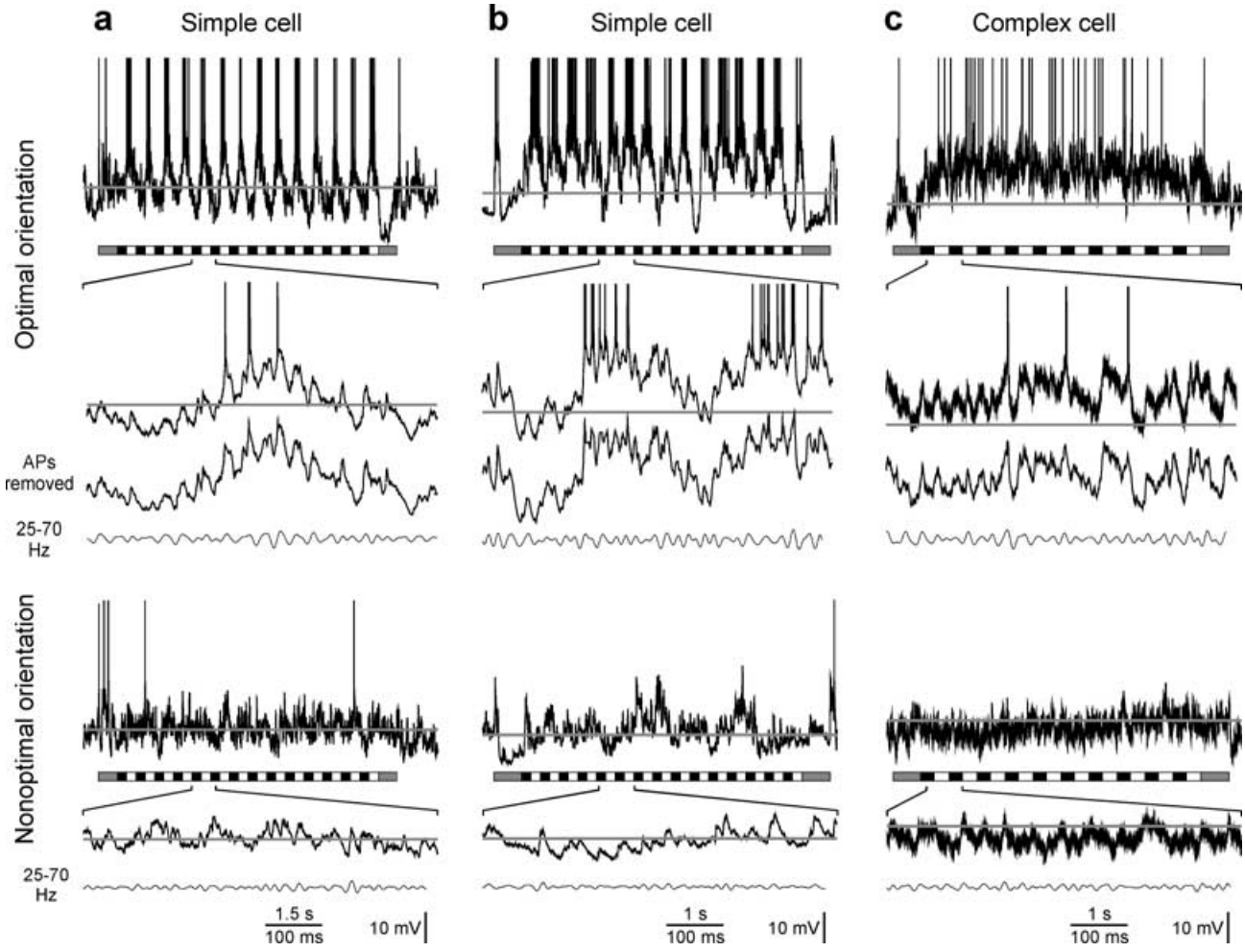

FIG. 1. High frequency fluctuations of the membrane potential in visual cortex neurons during responses to moving gratings of optimal (upper panels) and nonoptimal (lower panels) orientation. Data from (a and b) two cells with simple receptive fields and (c) a cell with complex receptive field. From top to bottom in each panel: membrane potential trace during the response to the moving grating; the bar indicates grating onset and end, the black–white pattern within the bar indicates beginning and end of movement and temporal frequency [2 Hz in (a), 3 Hz in (b) and 2 Hz in (c), note the different time scales in (a) and (b)]; a part of the membrane potential trace at higher temporal resolution; the same part of the membrane potential trace but with action potential removed (grey), and its γ-range component (lowermost in each panel). In this and the following figures, grey horizontal lines indicate the mean membrane potential during interstimulus intervals [−72.2 mV in (a), −79.8 mV in (b) and −59.4 mV in (c)]. Action potentials are truncated.

TABLE 1. Power of the γ-frequency range membrane potential fluctuations in visual cortical cells during responses to moving gratings of different orientation

	Power of the γ-frequency range membrane potential fluctuations at orientations relative to optimal (mV^2)							
	Optimal 0°	Oblique 5–75°	Non-optimal 90°	Oblique 105–165°	Null 180°	Oblique 195–255°	Non-optimal 270°	Oblique 285–345°
All cells ($n = 26$)								
Mean ± SEM	1.052 ± 0.129	0.494 ± 0.075	0.346 ± 0.039	0.393 ± 0.037	0.843 ± 0.102	0.355 ± 0.035	0.366 ± 0.044	0.431 ± 0.043
Median	0.566	0.274	0.251	0.334	0.561	0.257	0.258	0.379
P (vs.optimal)	–	< 0.001	< 0.001	< 0.001	< 0.001	< 0.001	< 0.001	< 0.001
Simple cells ($n = 9$)								
Mean ± SEM	1.659 ± 0.247	0.838 ± 0.188	0.498 ± 0.087	0.564 ± 0.077	1.260 ± 0.209	0.507 ± 0.081	0.536 ± 0.093	0.621 ± 0.088
Median	1.970	0.875	0.506	0.605	1.158	0.561	0.546	0.682
P (vs.optimal)	–	< 0.004	< 0.001	< 0.001	< 0.003	< 0.001	< 0.001	< 0.001
Complex cells ($n = 17$)								
Mean ± SEM	0.759 ± 0.127	0.323 ± 0.049	0.265 ± 0.036	0.306 ± 0.035	0.635 ± 0.100	0.276 ± 0.030	0.277 ± 0.043	0.335 ± 0.040
Median	0.503	0.233	0.207	0.233	0.373	0.211	0.214	0.237
P (vs.optimal)	–	< 0.001	< 0.001	< 0.001	< 0.015	< 0.001	< 0.001	< 0.001
P (simple vs. complex)	< 0.007	< 0.004	< 0.027	< 0.025	< 0.041	< 0.014	< 0.002	< 0.007

Averaged values were calculated as following. For each cell, orientation tuning curves of spike responses and γ-power were normalized to their maxima. The direction of stimulus movement which evoked maximal spike response (optimal) was defined as 0°. To average the data across cells in which different increments of stimulus orientation were used, the directions were pooled in eight groups, relative to the optimal: optimal (0°), from 15° to 75°, nonoptimal orientation (90°), from 105° to 165°, null direction (180°), from 195° to 255°, nonoptimal orientation (270°) and from 285° to 345°. If several orientations within a group were tested in a cell, as was often the case for the oblique to the optimal orientations, the responses were averaged, and that value was used for calculation of the average across cells.

constant or varies independently of the phase of the low frequency response, the coefficient is 0. In an ideal case, when the amplitude of high frequency oscillations during the positive phases of low frequency response is 1 and during the negative phases is 0.5, the phase-lock coefficient, calculated as above, is 752.

In order to obtain the averaged values of the strength of γ-frequency fluctuations of the membrane potential during presentation of stimuli in different orientation ranges apart from the optimal (Table 1) we did the following. For each cell, orientation tuning curves of spike responses and γ-power were normalized to their maxima. The optimal direction of stimulus movement was estimated from the spike responses and defined as 0°. To average the data across cells in which different increments of stimulus orientation were used, the directions were pooled in eight groups, relative to the optimal: optimal (0°), from 15° to 75°, nonoptimal orientation (90°), from 105° to 165°, null direction (180°), from 195° to 255°, nonoptimal orientation (270°) and from 285° to 345°. If several orientations within a group were tested in a cell, as was often the case for the oblique to the optimal orientations, the responses were averaged and that value was used for calculation of the average across cells.

For statistical evaluation of the data, *t*-tests and the Kolmogorov–Smirnov test were used. Data are presented as mean ± SEM if not stated otherwise.

Results

Neurons in the visual cortex respond to the presentation of moving gratings with changes in membrane potential and modification of the firing pattern. Both the membrane potential and the spiking rate can show different types of reactions: they are modulated at the temporal frequency of stimulation in some cells (Fig. 1a), express a general shift from the mean level for the whole period of stimulation but without a modulation at the temporal frequency of the presented grating in some other neurons (Fig. 1c), or show a combination of the modulation and the shift in the remaining cells (Fig. 1b). Modulation of the firing at the temporal frequency of stimulation is a hallmark of responses of neurons with simple receptive fields, while a general increase in the spiking rate with little modulation at the frequency of grating movement is characteristic of the complex cell responses. The spike response modulation index, which is defined as half of the peak-to-peak modulation divided by the mean increase in the spiking frequency (Dean & Tolhurst, 1983; Skottun *et al*., 1991), provides a quantitative measure for the classification of cortical neurons as simple or complex. The modulation index is >1 in simple cells but is <1 in cells with complex receptive fields.

In simple cells, presentation of optimally orientated gratings induced strong modulation of the membrane potential at the temporal frequency of stimulation (Fig. 1a and b). In addition to the slow rhythmic waves, which were synchronized to the periodicity of the moving grating, the membrane potential also fluctuated rapidly, in the γ-frequency range (25–70 Hz). These frequencies are at least 10 times higher than the temporal frequency of stimulation. In complex cells, γ-range fluctuations of the membrane potential were apparent during the depolarization shift of the membrane potential (Fig. 1c). In both simple and complex cells, the γ-frequency fluctuations of the membrane potential occurred throughout the response. The γ-frequency fluctuations were not uniform and periods of irregular weak fluctuations were intermingled with epochs during which fluctuation amplitudes rose up to ≈10 mV. During the responses to nonoptimaly orientated stimuli, both the slow and the rapid changes of the membrane potential were clearly weaker (Fig. 1a–c, lower panels).

To study the relationship between the stimulus optimality and the spectral composition of the membrane potential fluctuations we used three complementary approaches. First, we compared the power spectra of the membrane potential traces during the responses to optimal, nonoptimal and null stimulation. The simple cell in Fig. 2a shows a typical dependence of the response on the stimulus orientation. An optimal stimulus strongly modulates the membrane potential and the firing of the cell at the temporal frequency of stimulation. When the motion of the grating was changed to the opposite (null) direction, the modulation of the membrane potential became weaker and the spike response dropped to nearly 30%. A nonoptimally orientated grating failed to modulate the membrane potential of the

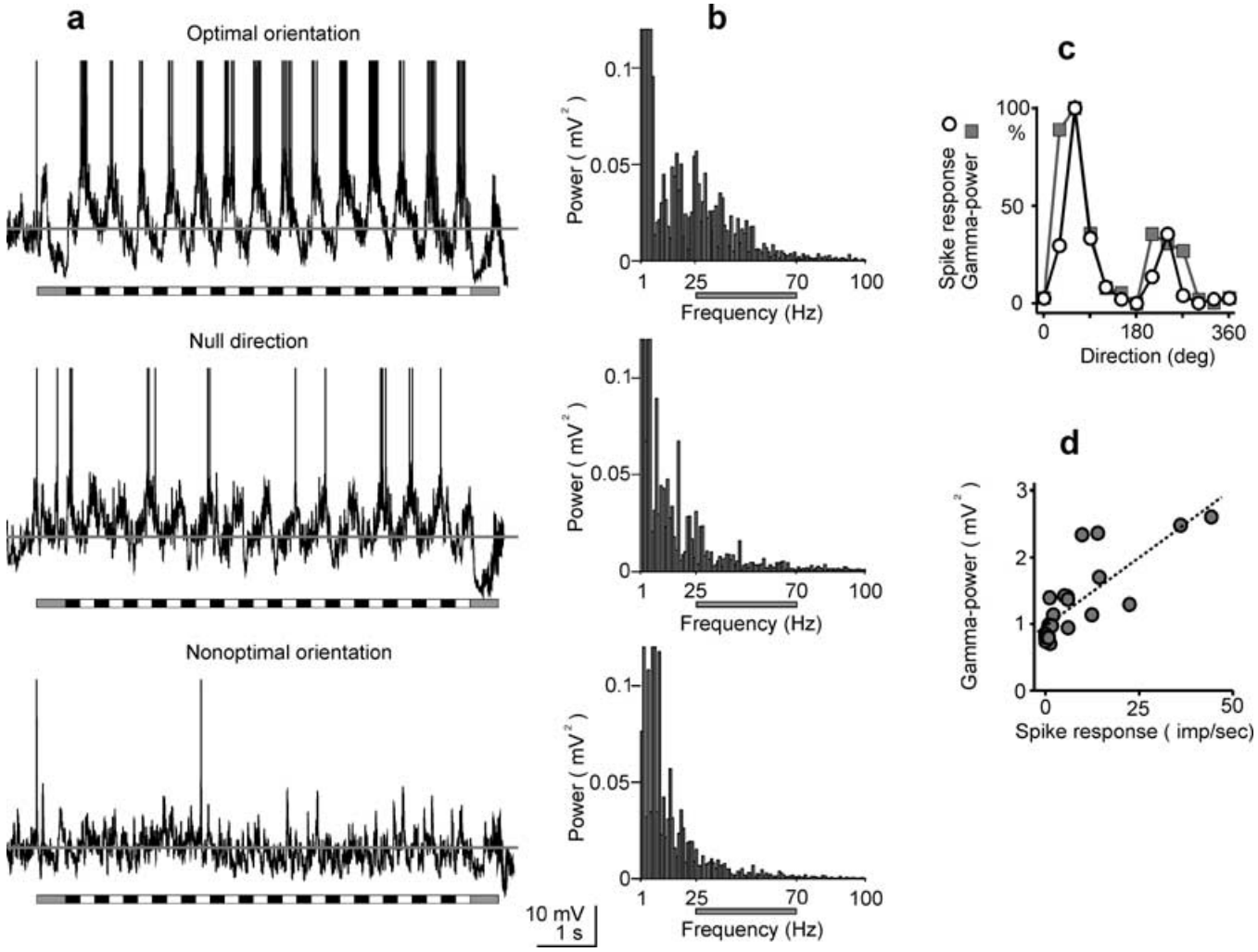

FIG. 2. The strength of γ-range oscillations of the membrane potential in a simple cell correlates with the stimulus optimality. (a) Responses of a simple cell to an optimally orientated grating moving in the optimal direction, in the opposite (null) direction and to a nonoptimally (orthogonal to the optimal) orientated grating. Grey horizontal lines indicate the mean membrane potential during interstimulus intervals (−73 mV in this cell). The bar below each trace shows grating onset and end, period of movement and temporal frequency (2 Hz). (b) Power spectra of the responses shown in (a). Initial bins are truncated. γ-frequency range (25–70 Hz) is indicated by the bars below each histogram. (c) Dependence of the spike count in the response (open circles) and of the strength of γ-frequency oscillations of the membrane potential (filled rectangles) on the direction of stimulus motion for the cell shown in (a). The strength of both spike responses and γ-power is normalized between 0 and 100% to facilitate comparison of tuning curves. (d) Correlation between the strength of the spike response and γ-power; same data as in (c). Grey line shows linear regression ($r = 0.81$, $n = 24$).

cell at the temporal frequency of stimulation and did not evoke action potentials (Fig. 2a). The power spectra of the responses show that fluctuations of the membrane potential in the γ-frequency range (25–70 Hz) were most pronounced during presentation of the optimal stimulus (Fig. 2b). This difference was representative of our sample of 26 cells as demonstrated in the scatter plot in Fig. 3a, which shows the relationship between the strength of γ-range oscillations of the membrane potential during optimal stimulation on the one hand, and nonoptimal as well as null stimulation on the other. All data points representing the nonoptimal orientation (red circles) are located above the main diagonal, as well as most of the data points representing the nonpreferred direction of grating movement (yellow diamonds). The difference in γ-power between the optimal and nonoptimal responses was larger than that between the optimal and null stimulation, but it was highly significant for both comparisons (1.05 ± 0.13 vs. 0.36 ± 0.04 and 1.05 ± 0.13 vs. $0.84 \pm 0.10\,\mathrm{mV}^2$; $P < 0.001$, paired-samples tests). Next, we extended this analysis to other orientations. For each cell, we calculated the orientation tuning of the spike responses and the tuning of the γ-power of the membrane potential fluctuations. In the cell in Fig. 2, the γ-power tuning had the same optimum and a similar shape to the tuning of the spike responses (Fig. 2c, squares and circles). Also, in other cells, presentation of moving gratings of any orientation outside the optimal range evoked significantly weaker γ-range oscillations than optimal stimuli. Group analysis of the whole sample of 26 cells, as well as separate analysis made for the simple ($n = 9$) and for the complex ($n = 17$) cells, revealed strongest fluctuations of the membrane potential in the γ-frequency range during presentation of gratings of optimal orientation (Table 1). In a third approach, we calculated the correlation between the γ-power of the membrane potential fluctuations and spiking during responses to stimuli of different orientations. This correlation was strong and highly significant for the cell in Fig. 2 ($r = 0.81$, $P < 0.001$), as well as in the majority of the other cells (23 out of 26). In 21 of these cells the correlation coefficient was >0.75 ($P < 0.001$). Taken together, these data demonstrate that changing the stimulus orientation led to parallel changes of the spike responses and the membrane

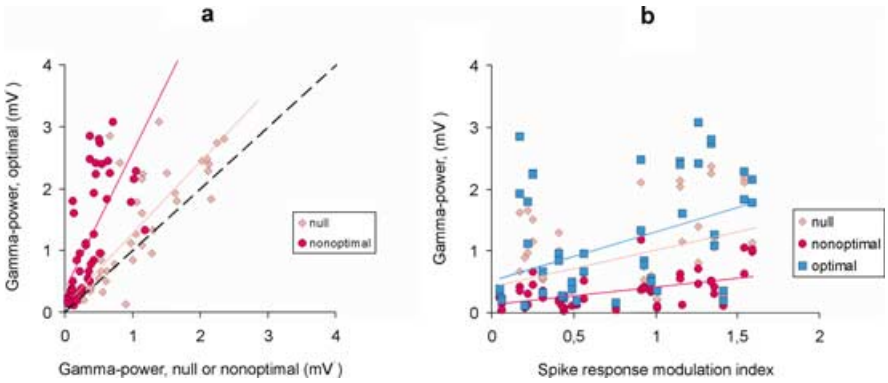

FIG. 3. Optimally orientated stimuli evoke strongest γ-range fluctuations of the membrane potential in visual cortex neurons. Summary data. (a) The strength of membrane potential oscillations in the γ-frequency range during optimal stimulation (ordinate) plotted against the γ-power in responses to grating movement in the null direction or at nonoptimal orientation (abscissa). Regression lines for the two data sets are shown in red and yellow. Diagonal shows equality line (interrupted). (b) Relationship between the strength of the γ-range fluctuations of the membrane potential oscillations (ordinates) during optimal (green), nonoptimal (red) and null stimulation (yellow) and spike response modulation index (abscissa). Regression lines for optimal ($r = 0.41$), nonoptimal ($r = 0.50$) and null stimulation ($r = 0.42$) are shown in the respective colour.

potential fluctuations in the γ-range: stronger spike responses were associated with a stronger γ-power.

Next, we assessed the possible difference in the strength of the γ-range membrane potential fluctuations between complex and simple cells. Because the strength of the γ-range fluctuations of the membrane potential depends on the stimulus orientation, the comparison between simple and complex cells was made separately for different ranges of stimulus orientation relative to the optimal. The strength of the γ-range fluctuations of the membrane potential was positively correlated with the spike response modulation index. The correlation for the optimal responses, for the responses to the nonpreferred direction of movement and to the grating of nonoptimal orientation, are illustrated in Fig. 3b. Under all three conditions of stimulation, the correlation was significant ($r = 0.41$, 0.42 and 0.49, respectively; $P < 0.01$ for all three correlations). Furthermore, significant difference between the simple and the complex cells in the strength of the γ-frequency fluctuations was found for all orientation ranges (Table 1).

Simple and complex cells also differed in the strength of the correlation between the γ-range fluctuations and the slow, stimulus-induced modulation of the membrane potential. This correlation was significant in all but two simple cells ($P < 0.05$ in seven out of nine cells), but only in few complex cells (four out of 17). That difference, however, is not surprising because in complex cells the modulation of the membrane potential at the temporal frequency of stimulation is weak or absent (Fig. 1; see also Carandini & Ferster, 2000).

We wondered whether there is also a phase relationship between the low frequency changes of the membrane potential and the strength (amplitude) of γ-range fluctuations. In theory, there are two possibilities. The first is an even distribution or random variation of γ-power, with no relationship to the phase of the low frequency changes. Alternatively, maxima of the amplitudes of γ-range oscillations may be locked to a certain phase of the low-frequency membrane potential fluctuations. To distinguish between these two possibilities, we have performed the following analyses. From the responses of a simple cell to an optimally orientated grating (Fig. 4a1) we extracted the spikes (Fig. 4a2), the low frequency (Fig. 4a3; 0.3–3 Hz) and the high frequency (Fig. 4a4; 25–70 Hz, γ-range) components of the membrane potential fluctuations. Response components of a certain frequency band were isolated by performing a fast Fourier transformation (FFT) of the membrane potential trace, then zeroing in the results all coefficients corresponding to the frequencies outside that given band, and then applying an inverse FFT. The spiking and the low-frequency component of the membrane potential response (a2 and a3) precisely followed the grating stimulus, as can be already seen in the original trace. More importantly, the γ-range fluctuations of the membrane potential occurred predominantly on the depolarizing peaks

TABLE 2. Correlation between the phase of low frequency membrane potential fluctuation and the strength of γ-range fluctuations

	Correlation coefficient at orientations which were:			Phase-lock coefficient at orientations which were:		
	Optimal	Non-optimal	Null	Optimal	Non-optimal	Null
All cells ($n = 26$)						
Mean ± SEM	0.243 ± 0.026	0.255 ± 0.015	0.235 ± 0.022	79.11 ± 9.39	68.11 ± 4.22	75.19 ± 8.12
Median	0.257	0.232	0.242	73.15	64.91	69.97
Simple cells ($n = 9$)						
Mean ± SEM	0.339 ± 0.046	0.323 ± 0.024	0.349 ± 0.024	120.07 ± 18.08	82.623 ± 6.916	111.423 ± 8.889
Complex cells ($n = 17$)						
Mean ± SEM	0.192 ± 0.027	0.219 ± 0.017	0.175 ± 0.026	57.435 ± 8.844	60.426 ± 4.884	56.004 ± 10.095
P (simple vs. complex)	< 0.004	< 0.017	< 0.001	< 0.002	< 0.022	< 0.002

Correlation coefficient between the low frequency component and the normalized amplitude of the envelope of the γ-frequency component of the membrane potential fluctuations. See Fig. 4 and related text for details of calculation. Phase-lock coefficient is the sum of products of a point-by-point multiplication of the normalized envelope of the high frequency component and low frequency component. See Methods and Fig. 4 for details.

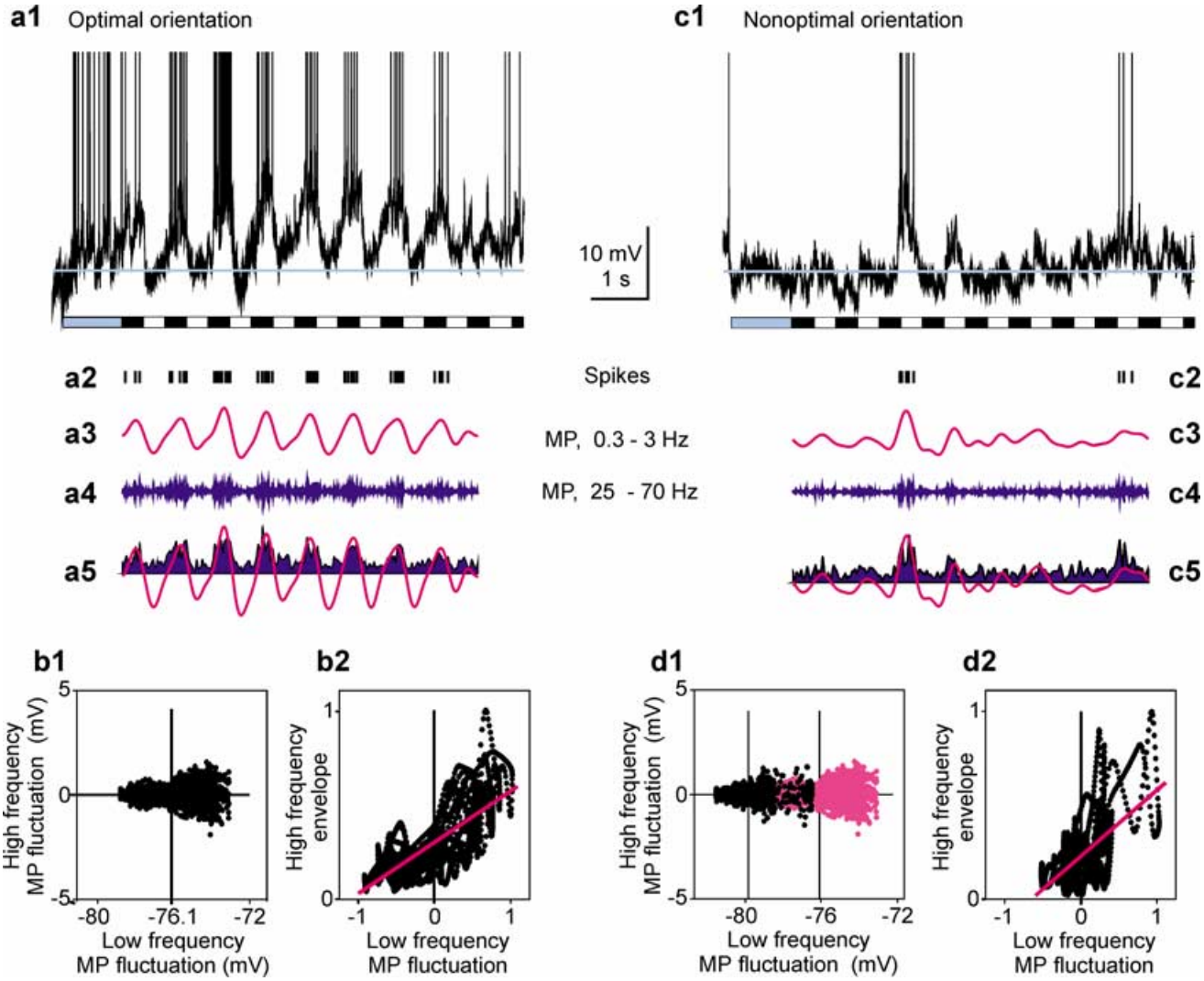

FIG. 4. Gamma frequency oscillations are strongest at the peaks of low frequency fluctuations of the membrane potential in a simple cell. Analysis of frequency composition of the membrane potential responses to the optimal (a and b) and nonoptimal (c and d) stimulation. (a1 and c1) Membrane potential traces. Mean membrane potential during interstimulus intervals −80.3 mV; other conventions as in Fig. 2a. Temporal frequency of the moving grating was 1.33 Hz. Spike responses (a2 and c2), low frequency (a3 and c3) and γ-range (a4 and c4) components of the membrane potential responses, extracted from traces in (a1) and (c1). (a5 and c5) Superposition of the normalized low frequency component (red) and the normalized envelope of the absolute value of high frequency component (blue) of the membrane potential response. (b1 and d1) Relationship between the low frequency and γ-range oscillations of the membrane potential; data from traces 3 and 4 in (a) and (c). Vertical lines show mean membrane potential during responses to the optimal (−76.1 mV) and nonoptimal (−79.8 mV) stimuli. Red symbols in (d1) repeat data from b1 for comparison. (b2,d2) Correlation between the amplitude of the envelope of oscillations in the γ-range and the phase of low frequency membrane potential oscillations. The scatter in (b2) is plotted using the data from (a5), $r = 0.73$; in (d2) data from (c5) are used, $r = 0.60$.

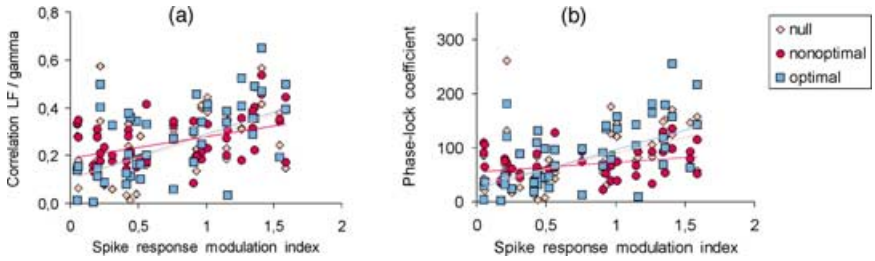

FIG. 5. Gamma-frequency oscillations are phase-locked to the peaks of low frequency fluctuations of the membrane potential in simple and complex cells. (a) Relationship between the spike response modulation index and the coefficient of correlation between the envelope of the high frequency fluctuations and the low frequency modulation of the membrane potential (for details see Fig. 4, b2 and d2). In each cell, the correlation coefficient was estimated separately from responses to optimal, nonoptimal and null stimulation. Note that coefficients >0.07 indicate a highly significant correlation ($P < 0.001$) because the number of data points for each correlation was 4096. The three data sets are shown with their regression lines (optimal, green rectangles and line, $r = 0.48$; nonoptimal, red circles and line, $r = 0.40$; null, yellow diamonds and line, $r = 0.54$). (b) Relationship between the spike response modulation index (abscissa) and the phase-lock coefficient (ordinate; see Materials and methods for details). Conventions as in (a). For the regression lines, $r = 0.52$ (optimal), $r = 0.30$ (nonoptimal) and $r = 0.48$ (null).

of the low frequency membrane potential modulation (Fig. 4, a3 and a4). We used several approaches to quantify this relationship. First, we plotted the amplitude of the high frequency component against the membrane potential value of the low frequency component, in a scatter diagram (Fig. 4b1). This scatter plot revealed a clear tendency for a larger amplitude of high frequency fluctuations at positive phases of the low frequency modulation. Second, we compared the envelope of the absolute values of the high frequency response component to the low frequency component (Fig. 4a5). The normalized amplitude of the envelope was significantly correlated with the normalized amplitude of the low frequency membrane potential fluctuations (Fig. 4b2; $r = 0.73$, $P < 0.001$). Third, we calculated the phase-lock coefficient, the sum of products of a point-by-point multiplication of the envelope of the high frequency component and low frequency component (see Materials and methods). For the example in Fig. 4a and b this coefficient was 121, indicating a strong association of large amplitude high frequency oscillations with the positive peaks of the slow membrane potential fluctuations. During nonoptimal stimulation (Fig. 4c) the spike response as well as the low frequency and the γ-range oscillations of the membrane potential were much weaker than those evoked by the optimal stimulus. Nevertheless, the phase relationship between the two components of the membrane potential fluctuations remained: γ-frequency oscillations of the highest amplitude occurred during occasional positive phases of the low frequency response component (Fig. 4: c3–c5, and d1 and d2). Notably, subthreshold peaks of the low frequency membrane potential fluctuations, which did not lead to spikes, were also associated with an increased amplitude of γ-range oscillations (Fig. 4, c3–c5). The mean membrane potential during the nonoptimal response was more negative than during the optimal stimulation (−80 vs. −76 mV). Interestingly, in the range of membrane potentials between −76 and −79 mV, which corresponded to the negative phases of the low frequency component during the optimal response but to the positive phases during the nonoptimal response, γ-range oscillations of the membrane potential were stronger during the peaks of nonoptimal response than during troughs of the optimal response (Fig. 4d1). Hence, the higher amplitude of γ-range oscillations of the membrane potential was associated with peaks of the low frequency components and not with the absolute value of the membrane depolarization. This observation is compatible with the notion that high-frequency fluctuations are imposed on the membrane potential by the synaptic input (see Discussion). In complex cells, modulation of the membrane potential at the temporal frequency of stimulation was less pronounced than in simple cells, and the low frequency fluctuations of the membrane potential often occurred with little or no relationship to the temporal frequency of the moving grating. Nevertheless, the γ-frequency membrane potential fluctuations had higher amplitude at the positive phases of low frequency fluctuations (data not shown).

During the optimal stimulation, a significant positive correlation ($P < 0.01$) between the envelope of the γ-range oscillations and the amplitude of low-frequency fluctuations of the membrane potential was found in all but three cells (23/26), and the phase-lock coefficient was positive in all but two cells (24/26). Also during the responses to stimuli of any other orientation, the correlation between the positive phases of the low frequency stimulation and the amplitude of the envelope of the γ-frequency fluctuations was significant in the majority of cells. When calculated from the responses to the optimal, nonoptimal and null stimulation, neither the averaged coefficients of correlation (0.24 ± 0.03, 0.26 ± 0.02 and 0.24 ± 0.02; see Table 2) nor the averaged phase-lock coefficients (79.1 ± 9.4, 68.1 ± 4.2 and 75.2 ± 8.1; see Table 2) differed significantly from one another. These data show that the association of largest amplitude γ-frequency oscillations with the peaks of stimulus-induced low frequency changes of the membrane potential was salient in responses to any orientation, despite a marked dependence of the response strength on the stimulus orientation. Although the phase-locking of the strongest γ-frequency fluctuations to the depolarization peaks of the low frequency membrane potential changes was apparent in the majority of cells in our sample, it was stronger in simple than in complex cells. This is indicated by the significant positive correlation between the spike response modulation index on the one hand, and the quantitative indices of the phase-locking on the other (Fig. 5a and b). Furthermore, both the correlation coefficients and the phase-lock coefficients were significantly larger in the simple than in the complex cells (Table 2).

Discussion

Our data demonstrate that (i) rapid, γ-range fluctuations of the membrane potential occur during responses to visual stimuli in both simple and complex cells, (ii) the strength of the γ-range fluctuations correlates with stimulus optimality and (iii) γ-frequency fluctuations of maximal amplitudes are phase-locked to the positive peaks of stimulus-induced low frequency changes of the membrane potential.

Contrary to previous studies, in which γ-range oscillations of the membrane potential were found predominantly in complex cells in the visual cortex (Jagadeesh *et al.*, 1992; Anderson *et al.*, 2000b), our quantitative analysis showed that, in the simple cells, fluctuations in the γ-range are not only present but are even stronger than in the neurons with complex receptive fields. This result is in accordance with the report on salient γ-frequency oscillations in chattering cells (Gray & McCormick, 1996), which represent a subpopulation of simple cells. Our analysis demonstrated that γ-frequency fluctuations of the membrane potential are characteristic for responses of the entire class of simple cells. Several lines of evidence indicate that the fluctuations of the membrane potential at frequencies >10 Hz might be of synaptic origin. First, their occurrence and frequency were preserved despite injection of hyperpolarizing current into the cell (Jagadeesh *et al.*, 1992; Bringuier *et al.*, 1997). Second, individual synaptic events contributing to each cycle of the membrane potential oscillations could be occasionally distinguished (Bringuier *et al.*, 1997). The oscillations could consist of trains of excitatory postsynaptic potentials or of alternating excitatory and inhibitory events (Bringuier *et al.*, 1997). Our data support this latter possibility because the falling phases of the membrane potential fluctuations were usually fast. Third, paired recordings revealed synchronous fluctuations of the membrane potential in the neighbouring cells, which have similar receptive fields and thus, most probably, receive overlapping inputs (Lampl *et al.*, 1999). Finally, relay cells in the lateral geniculate nucleus, which provide the major specific sensory input to the visual cortex, often generate high frequency oscillatory firing patterns during responses to visual stimulation (Neuenschwander & Singer, 1996). This oscillatory input is well suited to produce high frequency fluctuations of the membrane potential in visual cortical cells. At the same time, intrinsic resonant or oscillatory membrane properties of some neocortical neurons (Llinas *et al.*, 1991; Silva *et al.*, 1991; Jahnsen & Karnup, 1994; Gutfreund *et al.*, 1995; Hutcheon *et al.*, 1996; Hutcheon & Yarom, 2000), especially of chattering cells in the visual cortex (Gray & McCormick, 1996), might contribute to the generation of the cortical oscillatory activity as well.

Our analysis demonstrated that the strength of the γ-frequency fluctuations of the membrane potential correlates with stimulus optimality: stronger spike responses were associated with a stronger γ-power. This result is in accordance with earlier observations of strong

γ-range oscillations of the membrane potential during optimal stimulation (Jagadeesh *et al*., 1992; Gray & McCormick, 1996; Anderson *et al*., 2000b). Although the correlation between the γ-power of the membrane potential and the number of generated spikes as such does not prove a causal relationship between these two parameters, the following observations lend support to the possibility that an increase in the strength of high-frequency fluctuations of the membrane potential brings about an enhancement of the spike generation. An inverse relationship between the threshold of spike generation *in vivo* and the rate of the membrane potential rise (Azouz & Gray, 2000) implies that the threshold might be systematically lowered during the periods of high frequency fluctuations. Spike counts in response to identical stimuli were found to correlate with the γ-power immediately preceding the response (Azouz & Gray, 1999). *In vitro* studies have demonstrated that high frequency fluctuations of the membrane potential are most effective in producing trains of spikes with high temporal precision and may increase the spike count in responses of neurons with pronounced adaptation (Mainen & Sejnowski, 1995; Nowak *et al*., 1997; Stevens & Zador, 1998; Volgushev *et al*., 1998). During induced oscillations of the membrane potential, the number of spikes in response to the same test synaptic stimulus was higher when the membrane potential was modulated at higher frequency (Volgushev *et al*., 1998). The gain at which membrane depolarization is translated into trains of action potentials was found to correlate with the γ-power of the membrane potential, so that the same mean depolarization leads to more spikes when the γ-power is higher (Volgushev *et al*., 2002). Finally, a conservative procedure used in the present study, of the spike removal from the membrane potential trace, allows exclusion of the possibility of spurious enhancement of the γ-power by the presence of spike afterpotentials. Taken together, these data support the notion that γ-range fluctuations of the membrane potential enhance the spike generation in cortical neurons.

We have found that γ-range fluctuations of maximal amplitudes are phase-locked to the positive peaks of stimulus-induced low frequency changes in the membrane potential. Some earlier observations indicate that this kind of phase-locking may occur also in other brain structures, and thus provide an indirect support for our finding. In extracellular and some intracellular recordings, the amplitude of the oscillations at frequencies >15 Hz varied with the phase of the theta cycle of EEG in the hippocampus (Bragin *et al*., 1995; Ylinen *et al*., 1995) or with spontaneous fluctuations of the membrane potential in neocortical neurons (Steriade *et al*., 1996; Anderson *et al*., 2000b). Comparison of the relationship between the amplitude of the high frequency and the phase of the low frequency fluctuations during presentation of stimuli of different orientations extends these observations. Our data showed that, when the membrane potential troughs during the optimal responses and the peaks during the nonoptimal responses reached similar potential values, higher amplitudes of the γ-frequency fluctuations within that particular membrane potential range were observed on the peaks, i.e. during the nonoptimal responses (at peaks of the optimal responses the amplitudes of γ-frequency fluctuations were still higher). This observation demonstrates that stronger γ-range fluctuations of the membrane potential were associated specifically with the peaks, not just with the absolute value of the membrane depolarization. It also stresses the role of precisely temporally organized synaptic inputs in generation of the γ-frequency fluctuations of the membrane potential.

It was suggested by Von der Malsburg (1981, Internal Report, MPI Biophysical Chemistry, Göttingen) that the γ-range oscillations are involved in synchronization of neuronal activity and selection of cell assemblies by coherence of firing (for details see Eckhorn *et al*., 1988; Gray & Singer, 1989; Singer, 1993; Singer & Gray, 1995; Singer, 1999; Von der Malsburg, 1999). The demonstration of the capability of γ-frequency oscillations of the membrane potential to produce precisely timed patterns of cell discharges (Mainen & Sejnowski, 1995; Nowak *et al*., 1997) and to impose precise temporal windows for the integration of synaptic inputs (Lampl & Yarom, 1993; Volgushev *et al*., 1998) proves their suitability for that role. The dependence of the strength of γ-frequency fluctuations of the membrane potential on stimulus optimality may further expand the range of possible applications of the high frequency oscillations in stimulus encoding. Earlier studies demonstrated that response selectivity improves during transformation of membrane potential changes into trains of action potentials (Carandini & Ferster, 2000; Volgushev *et al*., 2000). Our recent results indicate a possible link between the selectivity improvement and the γ-range fluctuations of the membrane potential. Due to the enhancement of the spike generation, the γ-range fluctuations, being most effectively induced by optimal stimuli, may increase the spike yield during the optimal responses and thus contribute to the improvement of the spike response selectivity. Phase-locking of the strongest γ-range oscillations to the depolarization peaks of the low frequency membrane potential changes may bring further advantages. It has recently been suggested that a mechanism similar to stochastic resonance may be exploited in the visual cortex to detect weak signals and to enhance contrast invariance of orientation specificity (Troyer *et al*., 1998; Anderson *et al*., 2000a). However, the effect of stochastic high frequency noise has possible drawbacks. It helps to detect weak signals only when the relationships of the amplitudes of noise and signal to the threshold for spike generation are within a certain range (Ho & Destexhe, 2000). Outside that narrow range, stochastic high frequency noise prevents reliable transformation of the stimulus-imposed low frequency membrane potential changes into spike trains, and thus disturbs encoding of the temporal structure of a stimulus (Ho & Destexhe, 2000). Coupling of the high frequency fluctuation to the depolarization peaks of the low frequency signal allows this problem to be overcome and thus may expand the borders of applicability of stochastic resonance to the function of nerve cells. Such phase-locking provides visual cortex neurons with the possibility to exploit the advantages of the phenomenon of stochastic resonance in detection of weak signals but, at the same time, using a kind of amplitude modulation of the high frequency component, to preserve the temporal structure of the response in the low frequency range.

Acknowledgements

We are grateful to Marina Chistiakova, Klaus Funke and Thomas Mittmann for valuable discussions and comments. Supported by the Deutsche Forschungsgemeinschaft SFB 509 TP A5 to M.V.

Abbreviation

FFT, fast Fourier transformation.

References

Anderson, J.S., Lampl, I., Gillespie, D.C. & Ferster, D. (2000a) The contribution of noise to contrast invariance of orientation tuning in cat visual cortex. *Science*, **290**, 1968–1972.

Anderson, J., Lampl, I., Reichova, I., Carandini, M. & Ferster, D. (2000b) Stimulus dependence of two-state fluctuations of membrane potential in cat visual cortex. *Nature Neurosci.*, **3**, 617–621.

Azouz, R. & Gray, C.M. (1999) Cellular mechanisms contributing to response variability of cortical neurons in vivo. *J. Neurosci.*, **19**, 2209–2223.

Azouz, R. & Gray, C.M. (2000) Dynamic spike threshold reveals a mechanism for synaptic coincidence detection in cortical neurons in vivo. *Proc. Natl Acad. Sci. USA*, **97**, 8110–8115.

Bragin, A., Jando, G., Nadasdy, Z., Hetke, J., Wise, K. & Buzsaki, G. (1995) Gamma (40–100 Hz) oscillation in the hippocampus of the behaving rat. *J. Neurosci.*, **15**, 47–60.

Bringuier, V., Fregnac, Y., Baranyi, A., Debanne, D. & Shulz, D.E. (1997) Synaptic origin and stimulus dependency of neuronal oscillatory activity in the primary visual cortex of the cat. *J. Physiol. (Lond.)*, **500**, 751–774.

Carandini, M. & Ferster, D. (2000) Membrane potential and firing rate in cat primary visual cortex. *J. Neurosci.*, **20**, 470–484.

Dean, A.F. & Tolhurst, D.J. (1983) On the distinctness of simple and complex cells in the visual cortex of the cat. *J. Physiol. (Lond.)*, **344**, 305–325.

Eckhorn, R., Bauer, R., Jordan, W., Brosch, M., Kruse, W., Munk, M. & Reiboeck, H.S. (1988) Coherent oscillations: a mechanism of feature linking in the visual cortex. *Biol. Cybern.*, **60**, 121–130.

Engel, A.K., König, P., Kreiter, A.K. & Singer, W. (1991) Interhemispheric synchronization of oscillatory neuronal responses in cat visual cortex. *Science*, **252**, 1177–1179.

Frien, A. & Eckhorn, R. (2000) Functional coupling shows stronger stimulus dependency for fast oscillations than for low-frequency components in striate cortex of awake monkey. *Eur. J. Neurosci.*, **12**, 1466–1478.

Gray, C.M., Engel, A.K., König, P. & Singer, W. (1990) Stimulus-dependent neuronal oscillations in cat visual cortex: receptive field properties and feature dependence. *Eur. J. Neurosci.*, **2**, 607–619.

Gray, C.M. & McCormick, D.A. (1996) Chattering cells: Superficial pyramidal neurons contributing to the generation of synchronous oscillations in the visual cortex. *Science*, **274**, 109–113.

Gray, C.M. & Singer, W. (1989) Stimulus-specific neuronal oscillations in orientation columns of cat visual cortex. *Proc. Natl Acad. Sci. USA*, **86**, 1698–1702.

Gutfreund, Y., Yarom, Y. & Segev, I. (1995) Subthreshold oscillations and resonant frequency in guinea-pig cortical neurons: physiology and modelling. *J. Physiol. (Lond.)*, **483**, 621–640.

Ho, N. & Destexhe, A. (2000) Synaptic background activity enhances the responsiveness of neocortical pyramidal neurons. *J. Neurophysiol.*, **84**, 1488–1496.

Hutcheon, B., Miura, R.M. & Puil, E. (1996) Subthreshold membrane resonance in neocortical neurons. *J. Neurophysiol.*, **76**, 683–697.

Hutcheon, B. & Yarom, Y. (2000) Resonance, oscillation and the intrinsic frequency preferences of neurons. *Trends Neurosci.*, **23**, 216–222.

Jagadeesh, B., Gray, C.M. & Ferster, D. (1992) Visually evoked oscillations of membrane potential in cells of cat visual cortex. *Science*, **257**, 552–554.

Jahnsen, H. & Karnup, S. (1994) A spectral analysis of the integration of artificial synaptic potentials in mammalian central neurons. *Brain Res.*, **666**, 9–20.

König, P., Engel, A.K., Roelfsema, P.R. & Singer, W. (1996) How precise is neuronal synchronization? *Neur. Computation*, **7**, 469–485.

Lampl, I., Reichova, I. & Ferster, D. (1999) Synchronous membrane potential fluctuations in neurons of the cat visual cortex. *Neuron*, **22**, 361–374.

Lampl, I. & Yarom, Y. (1993) Subthreshold oscillations of the membrane potential: a functional synchronizing and timing device. *J. Neurophysiol.*, **70**, 2181–2186.

Livingstone, M.S. (1996) Oscillatory firing and interneuronal correlations in squirrel monkey striate cortex. *J. Neurophysiol.*, **75**, 2467–2485.

Llinas, R., Grace, A. & Yarom, Y. (1991) In vitro neurons in mammalian cortical layer 4 exhibit intrinsic oscillatory activity in the 10- to 50-HZ. frequency range. *Proc. Natl. Acad. Sci. USA*, **88**, 897–901.

Mainen, Z.F. & Sejnowski, T.J. (1995) Reliability of spike timing in neocortical neurons. *Science*, **268**, 1503–1506.

Neuenschwander, S. & Singer, W. (1996) Long-range synchronization of oscillatory light responses in the cat retina and lateral geniculate nucleus. *Nature*, **379**, 728–733.

Nowak, L.G., SanchezVives, M.V. & McCormick, D.A. (1997) Influence of low and high frequency inputs on spike timing in visual cortical neurons. *Cereb. Cortex*, **7**, 487–501.

Orban, G.A. (1984) *Neuronal Operations in the Visual Cortex*. Springer Verlag, Berlin, Heidelberg, New York, Tokyo.

Riehle, A., Grun, S., Diesmann, M. & Aertsen, A. (1997) Spike synchronization and rate modulation differentially involved in motor cortical function. *Science*, **278**, 1950–1953.

Salinas, E. & Sejnowski, T.J. (2000) Impact of correlated synaptic input on output firing rate and variability in simple neuronal models. *J. Neurosci.*, **20**, 6193–6209.

Silva, L.R., Amitai, Y. & Connors, B.W. (1991) Intrinsic oscillations of neocortex generated by layer 5 pyramidal cells. *Science*, **251**, 432–435.

Singer, W. (1993) Synchronization of cortical activity and its putative role in information processing and learning. *Annu. Rev. Psychol.*, **55**, 349–374.

Singer, W. (1999) Neuronal synchrony: a versatile code for the definition of relations? *Neuron*, **24**, 49–65.

Singer, W. & Gray, C.M. (1995) Visual feature integration and the temporal correlation hypothesis. *Annu. Rev. Neurosci.*, **18**, 555–586.

Skottun, B.C., Valois, R.L., Grosof, D.H., Moshon, J.A., Albrecht, D.G. & Bonds, A.B. (1991) Classifying simple and complex cells on the basis of response modulation. *Vision Res.*, **31**, 1079–1086.

Steriade, M., Contreras, D., Amzica, F. & Timofeev, I. (1996) Synchronization of fast (30–40 Hz) spontaneous oscillations in intrathalamic and thalamocortical networks. *J. Neurosci.*, **16**, 2788–2808.

Stevens, C.F. & Zador, A.M. (1998) Input synchrony and the irregular firing of cortical neurons. *Nature Neurosci.*, **1**, 210–217.

Troyer, T.W., Krukowski, A.E., Priebe, N.J. & Miller, K.D. (1998) Contrast-invariant orientation tuning in cat visual cortex: Thalamocortical input tuning and correlation-based intracortical connectivity. *J. Neurosci.*, **18**, 5908–5927.

Vaadia, E., Haalman, I., Abeles, M., Bergman, H., Prut, Y., Slovin, H. & Aertsen, A. (1995) Dynamics of neuronal interactions in monkey cortex in relation to behavioural events. *Nature*, **373**, 515–518.

Volgushev, M., Chistiakova, M. & Singer, W. (1998) Modification of discharge patterns of neocortical neurons by induced oscillations of the membrane potential. *Neuroscience*, **83**, 15–25.

Volgushev, M., Pernberg, J. & Eysel, U.T. (2000) Comparison of the selectivity of postsynaptic potentials and spike responses in cat visual cortex. *Eur. J. Neurosci.*, **12**, 257–263.

Volgushev, M., Pernberg, J. & Eysel, U.T. (2002) A novel mechanism of response selectivity of neurons in cat visual cortex. *J. Physiol. (Lond.)*, **540**, 307–320.

Von der Malsburg, C. (1999) The what and why of binding: The modeler's perspective. *Neuron*, **24**, 95–104.

Ylinen, A., Bragin, A., Nadasdy, Z., Jando, G., Szabo, I., Sik, A. & Buzsaki, G. (1995) Sharp wave-associated high-frequency oscillation (200 Hz) in the intact hippocampus: Network and intracellular mechanisms. *J. Neurosci.*, **15**, 30–46.